Polysulfone and Its Quaternary Phosphonium Derivative Composite Membranes with High Water Flux

ARTICLE *in* INDUSTRIAL & ENGINEERING CHEMISTRY RESEARCH · MARCH 2015

Impact Factor: 2.59 · DOI: 10.1021/acs.iecr.5b00416

5 AUTHORS, INCLUDING:

Ezzatollah Shamsaei
Monash University (Australia)
15 PUBLICATIONS **88** CITATIONS
SEE PROFILE

Ze-Xian Low
University of Bath
21 PUBLICATIONS **75** CITATIONS
SEE PROFILE

Xiaocheng Lin
Monash University (Australia)
22 PUBLICATIONS **297** CITATIONS
SEE PROFILE

I&EC research
Industrial & Engineering Chemistry Research

Article

pubs.acs.org/IECR

Polysulfone and Its Quaternary Phosphonium Derivative Composite Membranes with High Water Flux

Ezzatollah Shamsaei,[†] Ze-Xian Low,[†] Xiaocheng Lin,[†] Zhe (Jefferson) Liu,[‡] and Huanting Wang*[,†]

[†]Department of Chemical Engineering, Monash University, Clayton, Victoria 3800, Australia

[‡]Department of Mechanical and Aerospace Engineering, Monash University, Clayton, Victoria 3800, Australia

ABSTRACT: Tris(2,4,6-trimethoxyphenyl)polysulfonemethylene quaternary phosphonium chloride (TPQP-Cl) was blended with polysulfone (PSf) in different compositions to fabricate PSf/TPQP-Cl composite ultrafiltration membranes using the nonsolvent-induced phase separation method. The blending of polymers was confirmed by attenuated total reflectance infrared (ATR-IR) spectroscopy. Surface and cross-sectional morphologies of membranes were characterized using scanning electron microscopy (SEM). The SEM images showed that the PSf/TPQP-Cl membranes had a typical asymmetric structure. The X-ray photoelectron spectroscopy (XPS) and contact angle analysis revealed the enrichment of TPQP-Cl in the supporting layer of the membrane. In addition, water content, porosity, contact angle, pure water flux, and molecular weight cutoff were measured to study the influence of addition of TPQP-Cl. In particular, the addition of TPQP-Cl led to greatly increased water flux without significantly increased molecular weight cutoff; the PSf/TPQP-Cl membranes exhibited up to 7.3 times higher water flux than the pure PSf membrane at similar rejection properties. This work provides an effective way to tailor ultrafiltration membrane structure to achieve high flux while maintaining rejection properties.

1. INTRODUCTION

Ultrafiltration membranes that reject particles and macromolecules of 2−100 nm in size are widely used in the food, pharmaceutical, and biotechnological industries as well as water purification and wastewater treatment. These membranes are generally prepared by the phase inversion process (or known as the immersion precipitation technique). In this method, the polymer solution is cast on a glass plate (or other appropriate supports) with a casting knife, followed by immersion in a coagulation bath. Subsequently, phase inversion takes place by the exchange of solvent and nonsolvent, and an asymmetrical membrane with a thin nanoporous selective layer on top of a macroporous support is formed.[1] To obtain a desired membrane structure and properties, several approaches have been developed for tailoring surface properties and the microstructure of membranes. The most common approaches include surface treatment such as physical coating[2] or chemical grafting[3,4] of a hydrophilic material on the top of a formed membrane (postmodification), and blending of the membrane polymer with a hydrophilic agent.[5−13] These strategies have resulted in great improvement in membrane surface properties such as hydrophilicity and fouling resistance, but they have had limited success in achieving high water flux.

Our group has very recently introduced a new methodology for modifying ultrafiltration membrane structures to achieve greatly enhanced water permeability without sacrificing rejection property.[14,15] Ultrafiltration polymer membranes with unusually high water flux can be obtained using a polymer functionalized with hydrophobically ionizable groups as an additive; these membranes have a unique combination of pore wettability and charge density gradients. Specifically, a hydrophobic and charged polymer, tris(2,4,6-trimethoxyphenyl) polysulfonemethylene quaternary phosphonium chloride (TPQP-Cl) with a contact angle of 94° was added into poly(ether sulfone) (PES) having a contact angle of 75° (measured from dried dense PES film) to prepare PES/TPQP-Cl composite UF membrane.[14]

In the present work, we further investigate the applicability of the above methodology and explore how a different polymer component affects the overall membrane performance. Unlike PES, polysulfone (PSf, Figure 1) with the exactly same backbone as TPQP-Cl and a contact angle of 88° (measured from dried dense PSf film, more hydrophobic than PES) was chosen as the membrane matrix. Owing to its good mechanical, thermal, and chemical properties, PSf is commonly used in ultrafiltration membranes.[1] The phase inversion technique was used to prepare PSf/TPQP-Cl composite membranes. The effects of the amount of TPQP-Cl added into the casting solution on the membrane microstructure, surface wettability, water flux, and rejection properties were studied.

2. EXPERIMENTAL SECTION

2.1. Materials. Polysulfone (average Mw ∼ 35 000 by LS, average Mn ∼ 16 000 by MO, pellets), chloroform (anhydrous, ≥99%), paraformaldehyde (95%), trimethylchlorosilane (≥97%), stannic chloride (99%), 1-methyl-2-pyrrolidone (NMP, 99.5%), and tris(2,4,6-trimethoxyphenyl)phosphine were purchased from Sigma-Aldrich, Australia, and used without further purification.

2.2. Synthesis of Tris(2,4,6-trimethoxyphenyl)-polysulfonemethylene Quaternary Phosphonium Chloride (TPQP-Cl). Tris(2,4,6-trimethoxyphenyl)-polysulfonemethylene quaternary phosphonium chloride

Received: January 30, 2015
Revised: March 16, 2015
Accepted: March 18, 2015

DOI: 10.1021/acs.iecr.5b00416
Ind. Eng. Chem. Res. XXXX, XXX, XXX−XXX

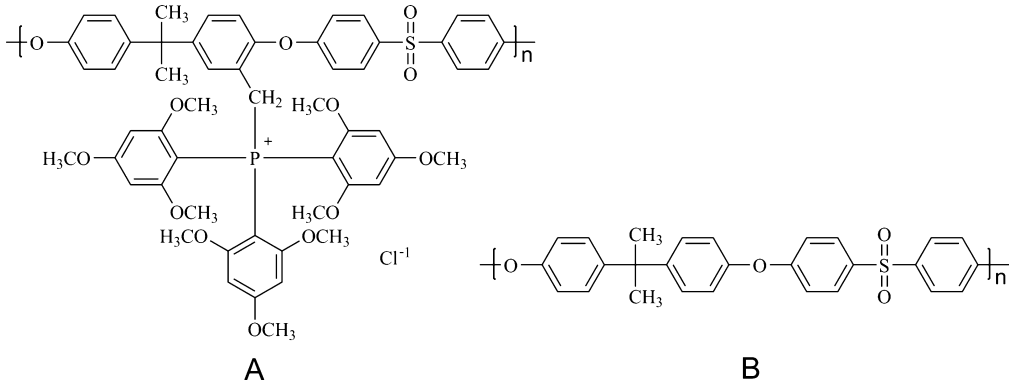

Figure 1. Molecular structure of (A) TPQP-Cl and (B) polysulfone.

Table 1. Compositions of Membrane Casting Solutions, Equilibrium Water Content and Porosity Values of the PSf and PSf/TPQP-Cl Composite Membranes at Various Compositions

membrane ID	PSf (wt %)	TPQP-Cl (wt %)	NMP (wt %)	EWC (%)	ε (%)	pore diameter from molecular weight cutoff (nm)
15% PSf	15	0	85	68.5	47.1	13
15% PSf/TPQP-Cl-9/1	13.5	1.5	85	79	53.9	13.5
15% PSf/TPQP-Cl-8/2	12	3	85	81.3	60.5	14.6
15% PSf/TPQP-Cl-7/3	11.5	4.5	85	85.5	65	15.3
18% PSf/TPQP-Cl-8/2	14.4	3.6	82	81	58	13.1

(TPQP-Cl) was synthesized according to the reported method.[16,17] Specifically, 3.39 g of paraformaldehyde and 12.3 g of trimethylchlorosilane were added to the polysulfone solution (5 g of PSf in 250 mL of chloroform) in a flask equipped with a reflux condenser and a magnetic stirrer, and then 0.6 g of stannic chloride was added dropwise. The reaction mixture was then stirred at 50 °C for 72 h. Subsequently, the reaction mixture was poured into absolute ethanol, and then white chloromethylated polysulfone (CMPSf) precipitated immediately. The precipitate was filtrated, washed thoroughly with ethanol, and dried under vacuum at room temperature for 12 h. 0.516 g of as-synthesized chloromethylated polysulfone was dissolved in 10 mL of 1-methyl-2-pyrrolidone (NMP), and then 0.8 g of tris(2,4,6-trimethoxyphenyl)phosphine was added. The reaction mixture was stirred at 80 °C for 12 h and then kept until further use.

2.3. Preparation of Membranes. Polysulfone (PSf) with an average molecular weight of 16 000 g/mol (Aldrich, MO, USA) was used as the membrane material. 1-Methyl-2-pyrrolidone (NMP) with an analytical purity of 99.5% and double deionized water were used as the solvent and the nonsolvent, respectively. As-synthesized TPQP-Cl was used as a polymer additive in the casting solution. Various PSf/TPQP-Cl/NMP solutions were prepared. Their compositions are presented in Table 1. Because TPQP-Cl itself did not have a good membrane formation property in the phase inversion process, pure TPQP-Cl membrane was not prepared. The viscosity of membrane casting solution was determined using a Haake Mars Modular Advanced Rheometer System. The polymer casting solution was prepared by dissolving PSf and TPQP-Cl in NMP at around 25 °C for 6 h with mechanical stirring at 200 rpm. The homogeneous solution was left stagnant until no bubbles were observed. Subsequently, the polymer solution was cast on a clean glass plate using a casting knife (Paul N. Gardner Co., Inc. USA) with a gap of 150 μm at room temperature (21−23 °C) and 30% humidity and immediately immersed in a coagulation bath of deionized water. After peeling off from the glass plate, the membranes were removed from the coagulation bath, rinsed with deionized water thoroughly to remove residual NMP, and kept in water before use.

2.4. Membrane Characterization. Scanning electron microscopy (SEM) (FEI Nova NanoSEM 450) was used for imaging the surface and cross-sectional morphologies of membranes. The membranes were fractured in liquid nitrogen, fixed on stubs with double-sided carbon tape and then sputter coated with roughly 2 nm platinum (Pt) layer to ensure good electrical conductivity. The images were recorded at an accelerating voltage of 5 kV with different magnifications. X-ray photoelectron spectroscopy (XPS) was performed with a Thermo Fisher X-ray photoelectron spectroscopy system (ESCALAB250). The X-ray radiation source was monochromatic Al Kα (1486.7 eV) and an electron takeoff angle of 90° relative to the sample plane was employed. FTIR spectra of the membranes were recorded using an attenuated total reflectance (ATR) Fourier transform infrared (FTIR) (PerkinElmer, USA) in the range of 500−4000 cm^{-1} at an average of 32 scans with a resolution of 4 cm^{-1}.

The static contact angles of the dried and wet membranes were measured at room temperature with a Model-PGX (FIBRO System AB, Sweden) analyzer. Double deionized water was used as the probe liquid in all measurements. The contact angle of all membranes was recorded at 30 s after a water drop was added onto the top surface of the membranes to get a steady reading. To get a reliable value, the contact angles were measured at five random locations for each membrane and the average number was recorded.

Water content of the membrane was determined after the membranes were soaked in deionized water for 24h at room temperature. Thereafter, the membranes were taken out and weighed followed by removing the surface water of membranes with Kimwipes Delicate Task Wipers. Then the wet membranes were placed in a vacuum oven at 65 °C for 6 h and the weights of the dried membranes were recorded. To ensure the reproducibility of data, the measurements were performed three times. The percent of water content (WC) and the

DOI: 10.1021/acs.iecr.5b00416
Ind. Eng. Chem. Res. XXXX, XXX, XXX−XXX

porosity (ε) of the membranes were calculated using eqs 1 and 2, respectively:

$$WC(\%) = \frac{(W_{wet} - W_{dry})}{(W_{wet})} \times 100 \quad (1)$$

$$\varepsilon(\%) = \frac{(W_w - W_d)}{V \times \rho} \times 100 \quad (2)$$

where W_{wet} and W_{dry} are the weight of the wet and dry membranes, respectively. V is volume of the membrane (cm^3) and ρ is the water density (g cm^{-3}). For the volume measurements of membranes, the thickness of the membranes were estimated by SEM image at different locations and the average was taken. The error was found to be within 2−3%.

2.5. Pure Water Flux and Molecular Weight Cutoff (MWCO) Measurements. Pure water flux of the membranes was determined at room temperature (21−23 °C) using a Sterlitech HP4750 dead-end stirred cell (Sterlitech Corporation, USA) with an inner diameter of 49 mm and an effective membrane area of 14.6 cm^2. The cell has a volume capacity of 300 mL and is attached to a 5.0 L dispensing vessel. Each membrane was first precompacted at 450 kPa for about 60 min until it reached a constant flux. Then the water flux was measured. The pure water flux was measured at 100, 200, 300, and 400 kPa by collecting the permeate on a digital balance (PA2102C, Ohaus) interfaced with a computer. The data from the balance was logged to a computer using a program written in LabVIEW.

Polyethylene glycol (PEG) with a molecular weight of 30, 100, 200, and 300 kDa (Analytical pure, Sigma-Aldrich) was dissolved in deionized water to prepare 1 g L^{-1} aqueous solutions to determine the MWCO and solute rejection of the membranes. Rejection measurements were performed at a pressure of 100 kPa. 20 mL of permeate was collected. The permeate and feed solution were both diluted by 10 times and then the concentration of each solution was measured via a total organic carbon analyzer (TOC-LCSH, Shimadzu, Japan). The PEG rejection was calculated from the measured feed (C_f) and permeate (C_p) concentrations by

$$R = \left(1 - \frac{C_p}{C_f}\right) \times 100$$

Three samples were analyzed under the same conditions for each membrane, and the standard deviation of rejection rate was about 4%. The pore size of the membrane was defined as the hydrodynamic diameter of PEG. The hydrodynamic radius of PEG can be calculated from the MWCO of the membrane by the following equation:[8]

$$\text{solute radius (nm)} = 0.0262\sqrt{\text{MW}} - 0.03$$

where MW is the lowest molecular weight of the PEG molecule that has a rejection of 90% in the ultrafiltration measurements.

3. RESULT AND DISCUSSION

3.1. Chemical Structure. Figure 2 shows the FTIR spectra of PSf, TPQP-Cl, and PSf/TPQP-Cl membranes prepared with different amounts of TPQP-Cl additive. The blending of PSf/TPQP-Cl membrane was confirmed by identifying the peaks corresponding to PSf and TPQP-Cl in the membrane. A typical spectrum of PSf can be seen in all membranes with characteristic peaks at 1144 (S═O symmetric stretching),

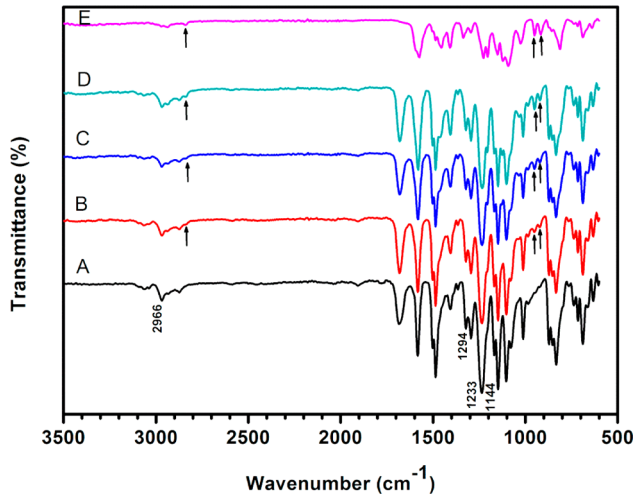

Figure 2. FTIR spectra of membranes prepared with a varied fraction of TPQP-Cl: (A) 15% PSf; (B) 15% PSf/TPQP-Cl-9/1; (C) 15% PSf/TPQP-Cl-8/2; (D) 15% PSf/TPQP-Cl-7/3; (E) TPQP-Cl.

1294 (S═O asymmetric stretching), and 1233 (C—O—C stretching), whereas peaks at 916, 950, and 2838 cm^{-1} are attributed to quaternary phosphonium groups. In the spectra of the PSf/TPQP-Cl blend membranes, with increasing TPQP-Cl content, three characteristic bands of quaternary phosphonium groups become more pronounced. Therefore, this confirms the presence of TPQP-Cl in the membranes.

3.2. Equilibrium Water Content (EWC) and Porosity (ε). As shown in Figure 3, the viscosity of the casting solution

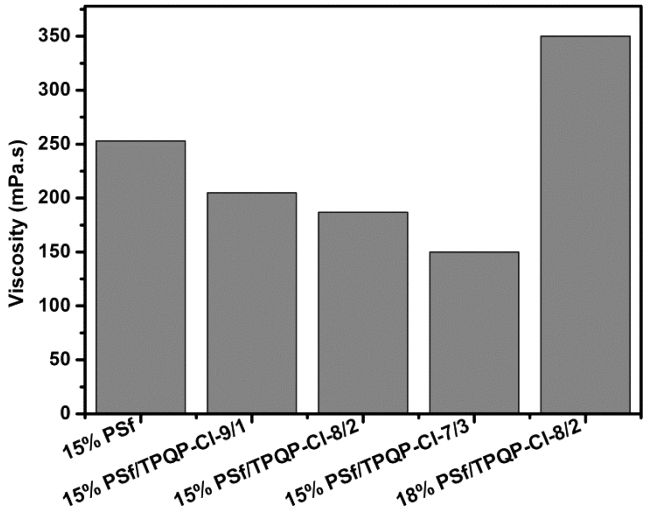

Figure 3. Viscosities of casting solutions containing varied fractions of PSf and TPQP-Cl (wt %) at shear rate of 100 s^{-1} and 23 °C.

decreases with increasing the fraction of TPQP-Cl. It is well-known that the viscosity of the casting solution and thermodynamic stability are two dominating factors in controlling the membrane porous structure and porosity during immersion precipitation process. The former is related to the mutual diffusivities between components in the system, and the latter is dependent on the phase equilibrium between them.[18] Because the addition of TPQP-Cl in the casting solution leads to the decrease in solution viscosity, the exchange rate between polymer solvent and nonsolvent during the phase inversion process would increase. This results in higher sublayer porosity

DOI: 10.1021/acs.iecr.5b00416
Ind. Eng. Chem. Res. XXXX, XXX, XXX−XXX

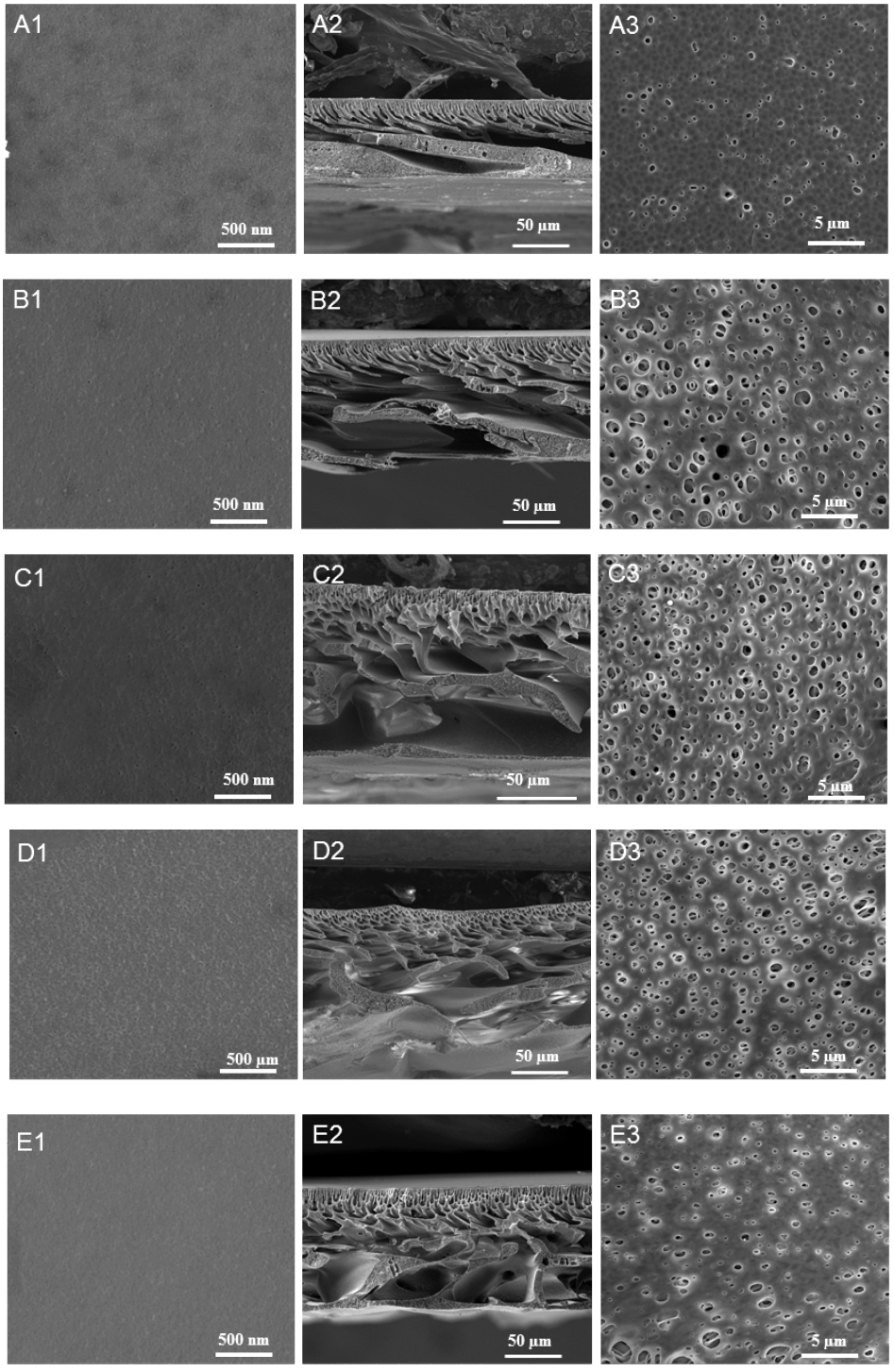

Figure 4. SEM images of top surface (A1−E1), bottom surface (A3−E3), and cross section (A2−E2) of membranes prepared with varied fraction of TPQP-Cl: (A1−A3) 15% PSf; (B1−B3) 15% PSf/TPQP-Cl-9/1; (C1−C3) 15% PSf/TPQP-Cl-8/2; (D1−D3) 15% PSf/TPQP-Cl-7/3; (E1−E3) 18% PSf/TPQP-Cl-8/2.

of the formed membranes. The porosity of PSf/TPQP-Cl 7/3 was 65%, which is the highest among all prepared membranes. Table 1 shows the effect of addition of TPQP-Cl in the casting solution on equilibrium water content (EWC) of different membranes. It was observed that the EWC of all membranes increases with increasing the fraction of TPQP-Cl in the casting solution. This is attributed to the increased porosity and hydration of quaternary phophonium groups.

3.3. Microstructure of Membranes. Figure 4 shows the surface and cross-sectional SEM images of the membranes. Similar to PES/TPQP-Cl membranes in our previous study,[14] all the PSf/TPQP-Cl membranes exhibit a typical asymmetrical ultrafiltration structure with a thin nanoporous top layer (skin) and a finger-like macrovoid supporting layer. There is no appreciable surface morphological change observed among the membranes with different fractions of the additive. This is in a good agreement with the data obtained from MWCO

DOI: 10.1021/acs.iecr.5b00416
Ind. Eng. Chem. Res. XXXX, XXX, XXX−XXX

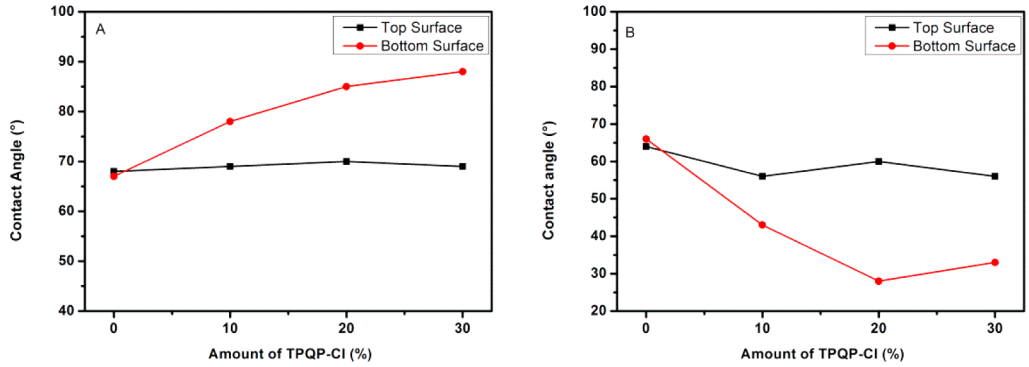

Figure 5. Contact angle of the top surface and bottom surface of 15% PSf membrane and 15% PSf/TPQP-Cl membranes in (A) dry state and (B) wet state, blended with different amounts of TPQP-Cl.

measurements. However, the cross-sectional images of the membranes prepared with the addition of TPQP-Cl (Figure 4) are different from the pristine PSf membrane. A comparison between these images in this figure shows that the addition of TPQP-Cl in the casting solution results in membranes with a more porous supporting layer and larger finger-like pores (especially at higher TPQP-Cl loading). Additionally, it can be seen that the thickness of the membranes increases with increasing the TPQP-Cl content. The greater thickness can be correlated to the greater porosity in the PSf/TPQP-Cl membrane as compared to the PSf membrane, considering the same polymer concentration of the casting solution being used for the PSf membrane and the PSf/TPQP-Cl membrane. This is consistent with porosity data where the higher TPQP-Cl content led to a higher porosity.

From the SEM images and porosity data, it can be seen that an increase in the concentration of polymer in the casting solution from 15% to 18% results in a decrease in the number of macrovoids. This is because decreased solvent and nonsolvent exchange rate, arising from increased viscosity in a higher polymer concentration, leads to suppression of the formation of macropores in the membrane.[19,20]

3.4. Contact Angle Measurement and XPS Analysis. The wettability of PSf/TPQP-Cl membranes was investigated by measuring their water contact angle. Figure 5A shows the contact angles of both top and bottom surfaces of dried membranes. With increasing the TPQP-Cl content, the water contact angle of the bottom surface significantly increases whereas the water contact angle of the top surface almost does not change. The higher water contact angle on the bottom surface can be explained by greater amount of hydrophobic unhydrated TPQP-Cl on the bottom surface. The distribution of the additive (TPQP-Cl) in the membrane is opposite to that observed in conventional membrane.[5,21,22] After immersion of the cast polymer solution in a water bath, unhydrated TPQP-Cl near the top surface of the solution would migrate from PSf matrix toward the glass plate so as to reduce interfacial energy between the polymer solution and the water bath. Note that the hydration of TPQP-Cl with quaternary phosphonium groups occurs more slowly as compared with the water-organic solvent (NMP) exchange rate, and TPQP-Cl remains hydrophobic during the rapid phase inversion process. The repulsive interactions between the hydrophobic TPQP-Cl and the water provide the driving force for the component migration to the bottom surface. However, owing to low polymer diffusivity, the migration of one polymer of a blend toward the bottom surface of the membrane to minimize the interfacial energy would not be extensive. Bearing this in mind, it is expected that the TPQP-Cl component moves partially apart into TPQP-Cl-rich and TPQP-Cl-poor phases, inducing gradients in TPQP-Cl content in the polymer matrix. This is consistent with XPS measurements that indicate the TPQP-Cl content on the bottom surface is higher than that of on the top surface for all PSf/TPQP-Cl blended membranes (Figure 6).

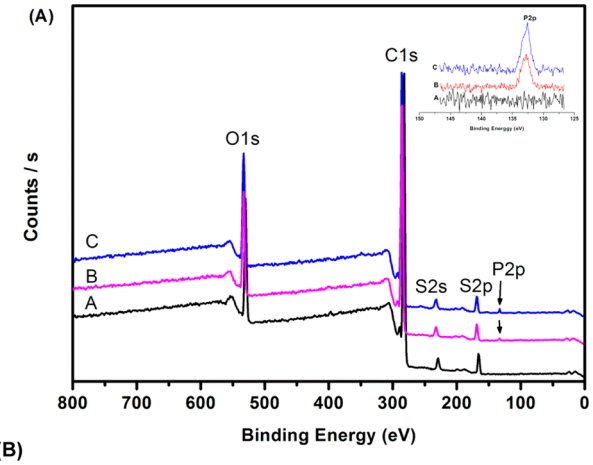

(B)

Sample		C (at %)	O (at %)	S (at %)	P (at %)
PSf		80.42	15.73	3.85	0
15% PSf/TPQP-Cl 9/1	Active layer	79.33	17.48	3.06	0.13
	Bottom layer	81.87	14.42	3.47	0.24
15% PSf/TPQP-Cl 8/2	Active layer	80.87	15.27	3.33	0.53
	Bottom layer	80.66	15.17	3.48	0.7
15% PSf/TPQP-Cl 7/3	Active layer	80.52	15.54	3.34	0.6
	Bottom layer	79.81	15.88	3.46	0.85

Figure 6. (A) XPS survey spectra of (A) the original PSf and PSf/TPQP-Cl membane at (B) active layer and (C) bottom layer; (B) Table showing atomic percentage calculated by XPS peak area for membrane with different TPQP-Cl contents.

DOI: 10.1021/acs.iecr.5b00416
Ind. Eng. Chem. Res. XXXX, XXX, XXX−XXX

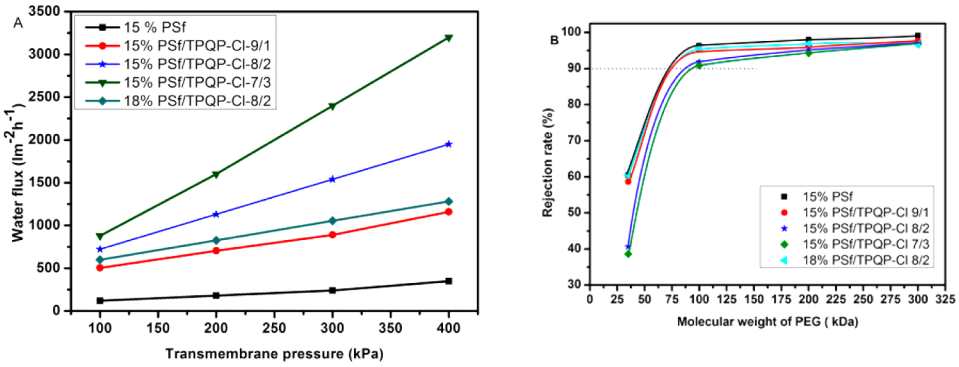

Figure 7. (A) Water flux of PSf and PSf/TPQP-Cl composite membranes as a function of transmembrane pressure. (B) Polyethylene glycol (PEG) molecular weight cutoff (MWCO) curves of all membranes studied in this work.

Because ultrafiltration membranes are normally fully hydrated in filtration processes, the water contact angle of wet membranes was also measured to evaluate the effect of the TPQP-Cl concentration on the pure water flux. The top surface of the wet membranes exhibits a slight decrease in their contact angle (from 64° to 56°) with increasing the TPQP-Cl content (Figure 5B). By contrast, the contact angle of the bottom surface of wet membranes drops drastically by increasing the amount of TPQP-Cl. As a result, the bottom surface of each wet PSf/TPQP-Cl membrane is much more hydrophilic than its top surface, whereas both surfaces of the PSf membrane have similar wettability. This can be elucidated by the fact that the TPQP-Cl-rich bottom surface becomes hydrophilic after full hydration of quaternary phosphonium groups. Therefore, unlike the conventional ultrafiltration membranes, there exists a wettability gradient, coinciding with a positive charge density gradient that increases from the top surface to the bottom surface in the PSf/TPQP-Cl membranes. This wettability gradient assists water permeation from the top surface to the supporting layer, which may contribute to enhanced water flow by promoting directional water movement.[23,24] Note that the water fluxes in PSf/TPQP-Cl membranes, as discussed below, are much higher than that of uniformly charged polymer membranes and of the membranes with a charged top surface.[7,25]

The increase in water contact angle of the bottom surface of the dried PSf/TPQP-Cl membrane is less pronounced compared to PES/TPQP-Cl membrane in our previous study.[14] This indicates that less TPQP-Cl migrates to the bottom surface in the phase inversion process for PSF/TPQP-Cl. This can be explained by the difference in wettability between PSf and PES. There is a greater difference in contact angle between TPQP-Cl and PES than that between TPQP-Cl and PSf, indicating a more pronounced segregation of TPQP-Cl in the phase inversion process for the PES/TPQP-Cl system. Therefore, the bottom surface of the PES/TPQP-Cl membrane is more hydrophobic than that of PSf/TPQP-Cl membrane. On the other hand, PES miscibility with TPQP-Cl is lower than PSf miscibility with TPQP-Cl, and thus enhanced segregation of TPQP-Cl makes the PES/TPQP-Cl bottom surface more hydrophobic.

3.5. Water Flux and Molecular Weight Cutoff. Pure water flux of the membranes was measured to evaluate the influence of polymer solution composition on the membrane permeability. The water fluxes as a function of transmembrane pressure are presented in Figure 7A. All the membranes showed a linear increase in water flux with increasing the transmembrane pressure. The gradient of these straight lines correlates with the hydraulic resistance during ultrafiltration. The resistance of the membrane decreases as the slope increases.[26,27] Due to the combined effects of increasing wettability gradient and porosity of the membrane structure, increasing TPQP-Cl concentration in the casting solution results in an increase in the slope. Compared with control PSf membrane, PSf/TPQP-Cl composite membranes exhibit much higher pure water flux. Pure water fluxes of the composite membranes with TPQP-Cl loading of 10 and 30 wt % were 4.2 and 7.3 times that of control PSf membrane, respectively. This can be explained by combined wettability and porosity effects as discussed in Sections 3.2, 3.3 , and 3.4, and our previous work.[14] Although the water flux of composite membrane increased with increasing the TPQP-Cl content, the memembrane with even a higher TPQP-Cl loading was not prepared because further increasing the TPQP-Cl content led to a reduction in mechanical strength of the membrane. It is worth mentioning that when the polymer concentration at a fixed PSf/TPQP-Cl ratio of 8:2 was increased from 15% to 18%, the water flux of the composite membrane decreased significantly. This is because the 18% polymer solution has a higher viscosity than the 15% polymer solution as shown in Figure 3, resulting in decreased TPQP-Cl gradient and smaller porosity.

The MWCO and pore size of the PSf and composite membranes were determined using polyethylene glycol (PEG) as a probe molecule, and the results are shown in Figure 7B. It can be seen from this figure that MWCO for control PSf membrane is about 62.5 kDa. The composite membranes showed a similar PEG rejection to control PSf membrane. The 90% PEG rejection rate was taken as MWCO value for each membrane, which was used to calculate the pore size of the active layer of the membrane. As it can be seen in Table 1, the pore size of the active layer does not significantly increase with increasing the content of TPQP-Cl. This is consistent with SEM observation on the membrane top surface.

The PES/TPQP-Cl membrane in our previous study exhibits a water permeability of 14.6 l m^{-2} h^{-1} kPa^{-1}, which is 35 times higher than that achieved by the pure PES membrane (0.46 l m^{-2} h^{-1} kPa^{-1}). This indicates that the water permeation enhancement in PES/TPQP-Cl membranes is much greater than that in PSf/TPQP-Cl. As discussed in previous sections, TPQP-Cl with PSf has higher miscibility than with PES. This is expected because TPQP-Cl is derived from PSf (Figure 1). A higher miscibility can result in smaller average pore size and subsequently lower water flux.[28] On the other hand, given a greater wetability difference between PES and TPQP-Cl, the

DOI: 10.1021/acs.iecr.5b00416
Ind. Eng. Chem. Res. XXXX, XXX, XXX−XXX

wettability gradient of the PES/TPQP-Cl membrane is more pronounced than that of PSf/TPQP-Cl membrane. Therefore, adding TPQO-Cl is an effective way to tailor microstructure and pore surface chemistry of ultrafiltration membrane to improve water flux at similar pore size.

4. CONCLUSION

The effect of adding TPQP-Cl into PSf ultrafiltration membrane on the porosity, water content, wettability, morphology, water flux and MWCO of the resultant membranes was investigated in comparison with TPQP-Cl/PES membranes. Like TPQP-Cl/PES composite membranes, the morphological analysis of the blend membranes showed that the connectivity of the pores was improved by addition of TPQP-Cl. XPS and contact angle analysis revealed that there exists a wettability gradient coupled with a positive charge density gradient that increases from the top surface to the bottom surface in the PSf/TPQP-Cl membranes. The porosity, water content and pure water flux of the PSf membranes were enhanced with increasing the TPQP-Cl content. In particular, the MWCO of the membrane did not increase much while the water flux was greatly improved. But the water flux enhancement observed in PSf/TPQP-Cl membranes was much less pronounced than that in PES/TPQP-Cl membranes due to a miscibility difference between the main component and the additive. This study indicates that adding a charged polymer additive with a switchable wettability before and after hydration leads to a unique membrane structure, favoring water permeation; the miscibility difference between the main component and the additive is a key parameter for effective engineering of ultrafiltration membranes with desirable structures for fast water permeation.

AUTHOR INFORMATION

Corresponding Author

*H. Wang. Tel.: +61399053449. E-mail: huanting.wang@monash.edu.

Notes

The authors declare no competing financial interest.

ACKNOWLEDGMENTS

This work is supported by the Australian Research Council (Project no. DP140101591). The authors acknowledge technical assistance from staff at Monash Center for Electron Microscopy of Monash University. Ezzatollah Shamsaei is also grateful to Monash University for a MGS and FEIPRS Scholarship.

REFERENCES

(1) Guillen, G. R.; Pan, Y.; Li, M.; Hoek, E. M. V. Preparation and characterization of membranes formed by nonsolvent induced phase separation: A review. *Ind. Eng. Chem. Res.* **2011**, *50*, 3798−3817.

(2) He, T.; Frank, M.; Mulder, M. H. V.; Wessling, M. Preparation and characterization of nanofiltration membranes by coating polyethersulfone hollow fibers with sulfonated poly(ether ether ketone) (SPEEK). *J. Membr. Sci.* **2008**, *307*, 62−72.

(3) Yu, H.; Zhang, Y.; Sun, X.; Liu, J.; Zhang, H. Improving the antifouling property of polyethersulfone ultrafiltration membrane by incorporation of dextran grafted halloysite nanotubes. *Chem. Eng. J.* **2014**, *237*, 322−328.

(4) Gao, Y.; Hu, M.; Mi, B. Membrane surface modification with TiO_2−graphene oxide for enhanced photocatalytic performance. *J. Membr. Sci.* **2014**, *455*, 349−356.

(5) Fan, Z.; Wang, Z.; Sun, N.; Wang, J.; Wang, S. Performance improvement of polysulfone ultrafiltration membrane by blending with polyaniline nanofibers. *J. Membr. Sci.* **2008**, *320*, 363−371.

(6) Ouradi, A.; Nguyen, Q. T.; Benaboura, A. Polysulfone−AN69 blend membranes and its surface modification by polyelectrolyte-layer deposit—Preparation and characterization. *J. Membr. Sci.* **2014**, *454*, 20−35.

(7) Mehta, A.; Zydney, A. L. Effect of Membrane Charge on Flow and Protein Transport during Ultrafiltration. *Biotechnol. Prog.* **2006**, *22*, 484−492.

(8) Peeva, P. D.; Million, N.; Ulbricht, M. Factors affecting the sieving behavior of anti-fouling thin-layer cross-linked hydrogel polyethersulfone composite ultrafiltration membranes. *J. Membr. Sci.* **2012**, *390−391*, 99−112.

(9) Rahimpour, A.; Madaeni, S. S. Improvement of performance and surface properties of nano-porous polyethersulfone (PES) membrane using hydrophilic monomers as additives in the casting solution. *J. Membr. Sci.* **2010**, *360*, 371−379.

(10) Shen, J.-n.; Li, D.-d.; Jiang, F.-y.; Qiu, J.-h.; Gao, C.-j. Purification and concentration of collagen by charged ultrafiltration membrane of hydrophilic polyacrylonitrile blend. *Sep. Purif. Technol.* **2009**, *66*, 257−262.

(11) Susanto, H.; Ulbricht, M. Characteristics, performance and stability of polyethersulfone ultrafiltration membranes prepared by phase separation method using different macromolecular additives. *J. Membr. Sci.* **2009**, *327*, 125−135.

(12) Wongchitphimon, S.; Wang, R.; Jiraratananon, R.; Shi, L.; Loh, C. H. Effect of polyethylene glycol (PEG) as an additive on the fabrication of polyvinylidene fluoride-co-hexafluoropropylene (PVDF-HFP) asymmetric microporous hollow fiber membranes. *J. Membr. Sci.* **2011**, *369*, 329−338.

(13) Zhao, Y.-H.; Zhu, B.-K.; Kong, L.; Xu, Y.-Y. Improving hydrophilicity and protein resistance of poly(vinylidene fluoride) membranes by blending with amphiphilic hyperbranched-star polymer. *Langmuir* **2007**, *23*, 5779−5786.

(14) Wang, K.; Lin, X.; Jiang, G.; Liu, J. Z.; Jiang, L.; Doherty, C. M.; Hill, A. J.; Xu, T.; Wang, H. Slow hydrophobic hydration induced polymer ultrafiltration membranes with high water flux. *J. Membr. Sci.* **2014**, *471*, 27−34.

(15) Lin, X.; Wang, K.; Feng, Y.; Liu, J. Z.; Fang, X.; Xu, T.; Wang, H. Composite ultrafiltration membranes from polymer and its quaternary phosphonium-functionalized derivative with Enhanced water flux. *J. Membr. Sci.* **2015**, *482*, 67−75.

(16) Gu, S.; Cai, R.; Luo, T.; Chen, Z.; Sun, M.; Liu, Y.; He, G.; Yan, Y. A soluble and highly conductive ionomer for high-performance hydroxide exchange membrane fuel cells. *Angew. Chem., Int. Ed.* **2009**, *48*, 6499−6502.

(17) Wang, K.; Zeng, Y.; He, L.; Yao, J.; Suresh, A. K.; Bellare, J.; Sridhar, T.; Wang, H. Evaluation of quaternary phosphonium-based polymer membranes for desalination application. *Desalination* **2012**, *292*, 119−123.

(18) Han, M.-J.; Nam, S.-T. Thermodynamic and rheological variation in polysulfone solution by PVP and its effect in the preparation of phase inversion membrane. *J. Membr. Sci.* **2002**, *202*, 55−61.

(19) Aerts, P.; Genne, I.; Kuypers, S.; Leysen, R.; Vankelecom, I. F. J.; Jacobs, P. A. Polysulfone−aerosil composite membranes: Part 2. The influence of the addition of aerosil on the skin characteristics and membrane properties. *J. Membr. Sci.* **2000**, *178*, 1−11.

(20) Alpatova, A.; Kim, E.-S.; Sun, X.; Hwang, G.; Liu, Y.; Gamal El-Din, M. Fabrication of porous polymeric nanocomposite membranes with enhanced anti-fouling properties: Effect of casting composition. *J. Membr. Sci.* **2013**, *444*, 449−460.

(21) Zhu, L.-P.; Xu, L.; Zhu, B.-K.; Feng, Y.-X.; Xu, Y.-Y. Preparation and characterization of improved fouling-resistant PPESK ultrafiltration membranes with amphiphilic PPESK-graft-PEG copolymers as additives. *J. Membr. Sci.* **2007**, *294*, 196−206.

(22) Razzaghi, M. H.; Safekordi, A.; Tavakolmoghadam, M.; Rekabdar, F.; Hemmati, M. Morphological and separation perform-

DOI: 10.1021/acs.iecr.5b00416
Ind. Eng. Chem. Res. XXXX, XXX, XXX−XXX

ance study of PVDF/CA blend membranes. *J. Membr. Sci.* **2014**, *470*, 547−557.
(23) Chen, Q.; Meng, L.; Li, Q.; Wang, D.; Guo, W.; Shuai, Z.; Jiang, L. Water transport and purification in nanochannels controlled by asymmetric wettability. *Small* **2011**, *7*, 2225−2231.
(24) Zheng, Y.; Bai, H.; Huang, Z.; Tian, X.; Nie, F.-Q.; Zhao, Y.; Zhai, J.; Jiang, L. Directional water collection on wetted spider silk. *Nature* **2010**, *463*, 640−643.
(25) Ager, K.; Latulippe, D. R.; Zydney, A. L. Plasmid DNA transmission through charged ultrafiltration membranes. *J. Membr. Sci.* **2009**, *344*, 123−128.
(26) Amirilargani, M.; Saljoughi, E.; Mohammadi, T. Improvement of permeation performance of polyethersulfone (PES) ultrafiltration membranes via addition of Tween-20. *J. Appl. Polym. Sci.* **2010**, *115*, 504−513.
(27) Wang, Y.; Su, Y.; Sun, Q.; Ma, X.; Ma, X.; Jiang, Z. Improved permeation performance of Pluronic F127−polyethersulfone blend ultrafiltration membranes. *J. Membr. Sci.* **2006**, *282*, 44−51.
(28) Kim, J. H.; Kim, C. K. Ultrafiltration membranes prepared from blends of polyethersulfone and poly(1-vinylpyrrolidone-co-styrene) copolymers. *J. Membr. Sci.* **2005**, *262*, 60−68.

DOI: 10.1021/acs.iecr.5b00416
Ind. Eng. Chem. Res. XXXX, XXX, XXX−XXX